Detection of Kinase Translocation Using Microfluidic Electroporative Flow Cytometry

Jun Wang, Ning Bao, Leela L. Paris, Hsiang-Yu Wang, Robert L. Geahlen and Chang Lu[a)]
Departments of Agricultural and Biological Engineering, Department of Medicinal Chemistry and Molecular Pharmacology, School of Chemical Engineering, Birck Nanotechnology Center and Bindley Bioscience Center, Purdue University, West Lafayette, Indiana 47907, USA.

I. INTRODUCTION

Translocation of a protein between different subcellular compartments is a common event during signal transduction in living cells. Integrated signaling cascades often lead to the relocalization of protein constituents such as translocations between the cytoplasm and the plasma membrane or nucleus. Such events can be essential for the activation/deactivation and biological function of the protein. The protein-tyrosine kinase, Syk, is a prime example of a protein that translocates to the B cell receptors (BCR) in plasma membrane as part of its role in signal transduction upon stimulation.

Determination of the translocation of kinases within cells has been traditionally carried out using methods such as subcellular fractionation/Western blotting or imaging of a few cells where only average information was gathered. Flow cytometry has been the tool of choice for single cell studies within cell populations of relatively large sizes. However, conventional flow cytometry is intrinsically insensitive to the subcellular location of the probed protein. Laser scanning cytometry (LSC) quantifies nuclear/cytoplasmic distribution of a fluorescent labeled protein based on solid phase cytometry technique [1-3] at a throughput only at ~100 cells/s. A recently developed complementation assay for protein translocation (CAPT) demands complex biological molecule manipulation [4]. Simple and robust high-throughput methods for examining intracellular translocation at the single cell level are highly demanded for mechanistic studies and clinical applications.

Here we demonstrate a new high-throughput technique, which we refer to as electroporative flow cytometry (EFC), to observe the translocation of the kinase Syk from the cytoplasm to plasma membrane at the level of the cell population with information gathered from single cells. Electroporation occurs when cells experience an electrical field with the intensity beyond a certain threshold. During electroporation the electrical field opens up pores in the cell membrane. Such pores allow the release of intracellular materials into the surrounding solution [5-7]. In this study, we found that the amount of SykEGFP left in the cells after electroporation was related to whether or not translocation of Syk to the plasma membrane occurred. Microfluidic EFC was able to detect the translocation of Syk and provide characteristics of the entire cell population in terms of the release of the intracellular kinase. We envision that the same mechanism can be extended to the detection of translocations involving other kinases and cell types.

II. EXPERIMENT

1. Microchip fabrication.

The general information about PDMS microfluidic chip fabrication based on standard soft lithography was provided in our previous publication[8]. The dimensions of

fabricated microfluidic channels is showed in Figure 1 (a). The depth of the microfluidic device was uniformly 33 μm.

2. Cell sample preparation.

Syk- and Lyn-deficient (Syk/Lyn-deficient)[9] chicken DT40 B cells (DT40-Syk$^-$-Lyn$^-$) and SykEGFP-DT40-Syk$^-$-Lyn$^-$ cell lines were produced as described before [10]. Cells can be stimulated with 50 μg/ml goat anti-chicken immunoglobulin M (IgM) antibody (Bethyl Laboratories, Montgomery, TX) for 1 h at 20 ℃.

To establish a negative control, both stimulated and unstimulated DT40-Syk$^-$-Lyn$^-$ were labeled with a fluorogenic dye, calcein AM (Invitrogen, Carlsbad, CA) after the above procedure for 1 h stimulation or incubation. The labeling was done by incubating the cells with calcein AM at a concentration of 20 ng/ml for 10 min.

3. Microchip operation and signal detection.

The setup of the apparatus is shown in Figure 1. The microfluidic EFC device was mounted on an inverted fluorescence microscope (IX-71, Olympus, Melville, NY) with a 40X dry objective (NA=0.60). A high voltage power supply (PS350, Stanford Research Systems, Sunnyvale, CA) was used to generate a constant direct current (DC) voltage in between the sample and the outlet reservoirs.

An air-cooled 100mW argon ion laser (Spectra-Physics, Mountain View, CA) at 488 nm was applied as the excitation source for laser-induced fluorescence that was recorded by LabView software (National Instruments, Austin, TX). The data were processed by programs written in MATLAB to extract histograms of the fluorescence from a cell population. The data were presented in 4 decades (from 0.001 to 10 V) logarithmic histograms with 256 channels. The voltage signal ranging from 1 mV to 10 V was converted to 4 decade logarithmic voltage scale and then 256 scale channels.

4. Conventional flow cytometry.

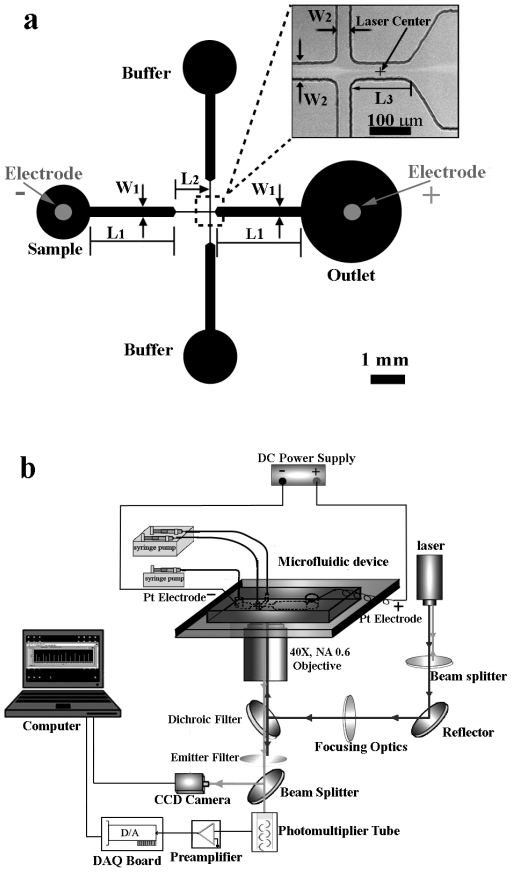

Figure 1. (**a**) The layout of the microfluidic chip. The width varied in the horizontal channel with W_1 of 300 μm and W_2 of 33 μm. The length of the narrow section L_2 was set as either 1 or 2 mm in different experiments. The other sections in the horizontal channel had a length of 2.5 mm for L_1 and 150 μm for L_3. The depth of the microfluidic channels was uniformly 33 μm. The laser detection point was positioned at the center of the horizontal channel after hydrodynamic focusing. In the inset image, the fluorescent trail was left by SykEGFP-DT40-Syk$^-$-Lyn$^-$ cells when the ratio between the flow rate in one of the two vertical channels and that in the horizontal channel was 3:1. (**b**) A schematic illustration of the setup of the microfluidic electroporative flow cytometry apparatus.

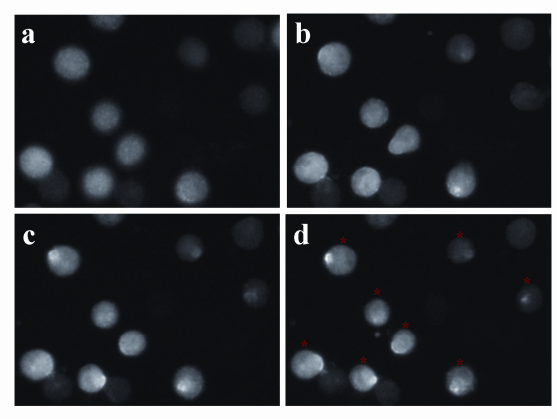

Figure 2. The fluorescent images showing capping of SykEGFP at the plasma membrane. SykEGFP was redistributed to the plasma membrane after stimulation with anti-IgM antibody at room temperature for 5 min (**a**), 30 min (**b**), 60 min (**c**) and 90 min (**d**). The cells labeled by red asterisks in (d) were considered the ones with capping. The percentage of cells with capping was 81±3% (enumerated in three separate experiments by one observer with the results of 396/470, 462/575, and 388/497).

We also conducted screening of the chicken DT40 cells (stimulated and unstimulated) using a commercial flow cytometer with 488 nm excitation and FL-1 525 nm BP emission filter (Cytomics^{TM} FC 500 flow cytometer, Beckman Coulter, Inc., Fullerton, CA) at the Purdue University Flow Cytometry Laboratories. For each run, around 10000 cells were screened for fluorescence intensity.

5. Fluorescence intensity calibration.

We used Molecules of Equivalent Soluble Fluorophores (MESF) units to quantify the fluorescence intensity from single cells when microfluidic EFC was used [11, 12]. The mean percentage of EGFP or calcein of a cell population, P_{EGFP}, (by assuming that SykEGFP-DT40-Syk$^-$-Lyn$^-$ population without electroporation has a mean percentage of 1 and DT40-Syk$^-$-Lyn$^-$ population has a mean percentage of 0) was calculated using following formulae (Φ=fluorescence quantum yield, ε=extinction coefficient, A=absorbance, peak A_{EGFP}=489 nm, peak $A_{Fluorescein}$=495 nm, V=average cell volume, $EGFP_{mean}$= the population mean MESF value of EGFP fluorescence signal interpolated from the standard curve (Figure 5 in Supporting Information),

$$[EGFP]= EGFP_{mean}\times B\times K/V \quad (1)$$

Where $B=\Phi_{EGFP}\times\varepsilon_{EGFP}\times A_{EGFP:488nm}/A_{EGFP:484nm}/(\Phi_{Fluorescein}\times\varepsilon_{Fluorescein}\times A_{Fluorescein:488nm}/A_{Fluorescein:490nm})$

From the standard curve, K= moles fluorescein/relative fluorescent units. $[EGFP]_{control}$ is the value for DT40-Syk$^-$-Lyn$^-$ population (without EGFP tagging and without electrical field), $[EGFP]_{E=0}$ is the value for SykEGFP-DT40-Syk$^-$-Lyn$^-$ population without the electrical field. By assuming constant B, K and V under different electric field, P_{EGFP} of a cell population can be calculated to be

$$P_{EGFP} = \frac{([EGFP]\text{-}[EGFP]_{Control})}{([EGFP]_{E=0}\text{-}[EGFP]_{Control})}\times 100\% \quad (2)$$

The average percentage of calcein in a given cell population was calculated using the same method.

III. RESULTS AND DISCUSION

The design and setup of the microfluidic EFC device is shown in Figure 1. A new microfluidic electroporation technique based on constant DC voltage was applied here [7, 13]. The horizontal channel was composed of two wide sections (W_1 = 300 μm) and one narrow section (W_2= 30 μm) with the depth of the whole channel being uniform (Figure 1a). The field strength in the narrow section was approximated to be 10 times

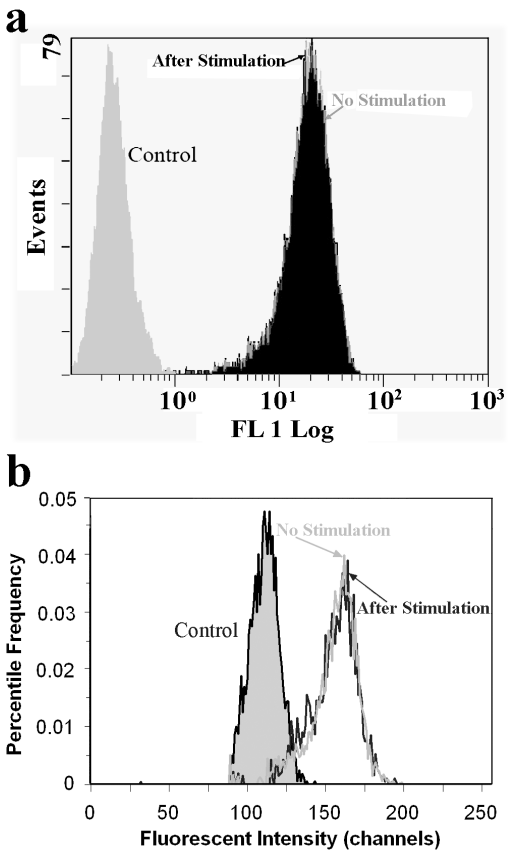

Figure 3. The histograms of the fluorescent intensity of SykEGFP-DT40-Syk$^-$-Lyn$^-$ cells with and without stimulation by anti-IgM antibody and the DT40-Syk$^-$-Lyn$^-$ cells (the control). (**a**) Histograms obtained by Cytomics FC 500 Flow cytometer (grey: without stimulation; black: stimulated by anti-IgM; Grey: the control, DT40-Syk$^-$-Lyn$^-$ cells without EGFP labeling). The data generated by dead cells (determined based on scatter properties) were excluded from the analysis. (**b**) Analysis of the same samples as in (**a**) in the microfluidic device (with the voltage at 0). To eliminate the effect of different cell sample sizes on the shape of the histograms, the distributions were normalized to have percentile frequency for the y-axis.

higher than the field strength in the wide sections according to Ohm's law, We have shown that when the overall voltage is in the right range, electroporation exclusively occurs in the narrow section since the field intensity in the wide sections are too weak to compromise the cell membrane [7, 13]. The velocity of cells here was determined mostly by the infusion rate of the syringe pump.

In our experiment, we applied SykEGFP-expressing chicken DT40 cells lacking both Syk and Lyn to ensure that the localization of Syk at the plasma membrane lasted long enough for us to finish the tests. The cells were stimulated at room temperature (20°C) by anti-IgM antibody. Fluorescence images were taken at timed intervals of 0.5 h. Figure 2 shows that the cells started to show patches and caps of fluorescent clusters at 5 min (Figure 2a). Within 60 min the vast majority of cells had a single cap at one pole. Figure 3 shows the event frequency versus the fluorescence intensity for the cell populations with and without anti-IgM stimulation. With a commercial flow cytometer the mean fluorescence intensity of the cell population with translocation (after anti-IgM stimulation) was 19.6 compared to 19.2 for the cell population without stimulation, on a 0.1 to 1000 logarithmic relative brightness scale (10,000 cells in each population). The histograms of the two cell populations overlapped very well. When screening the cells in our microfluidic device, the two cell populations (2,000~3,000 cells in each population) with and without stimulation also overlapped with the mean channels being 159 and 160, respectively. The results indicate that the translocation cannot be detected with conventional flow cytometry approach using either a commercial flow cytometer or our microfluidic flow cytometer.

We applied microfluidic EFC to analyze the cell populations with and without anti-IgM stimulation, under varying voltages across the sample and outlet reservoirs. Figure 4 shows the mean fluorescence intensity of the cell population plotted against the field intensity for all the three experiments. It was found that the optimal field intensities for

detecting translocation to the plasma membrane in a cell population was around 700 and 800 V/cm with a duration of 120 ms or 1000 V/cm with a duration of 60 ms (significantly different at P<0.01).

We have also taken both phase contrast and fluorescent images of the cells after being processed in the microfluidic EFC device. The cell size after the tests became increasingly larger when the field intensity increased, due to the influx of the surrounding solution during electroporation. The residual fluorescence from the cells decreased with increasing field intensity. No significant fragmentation of the plasma membrane was observed. There was some sign of possible membrane fragments only at the highest field intensity

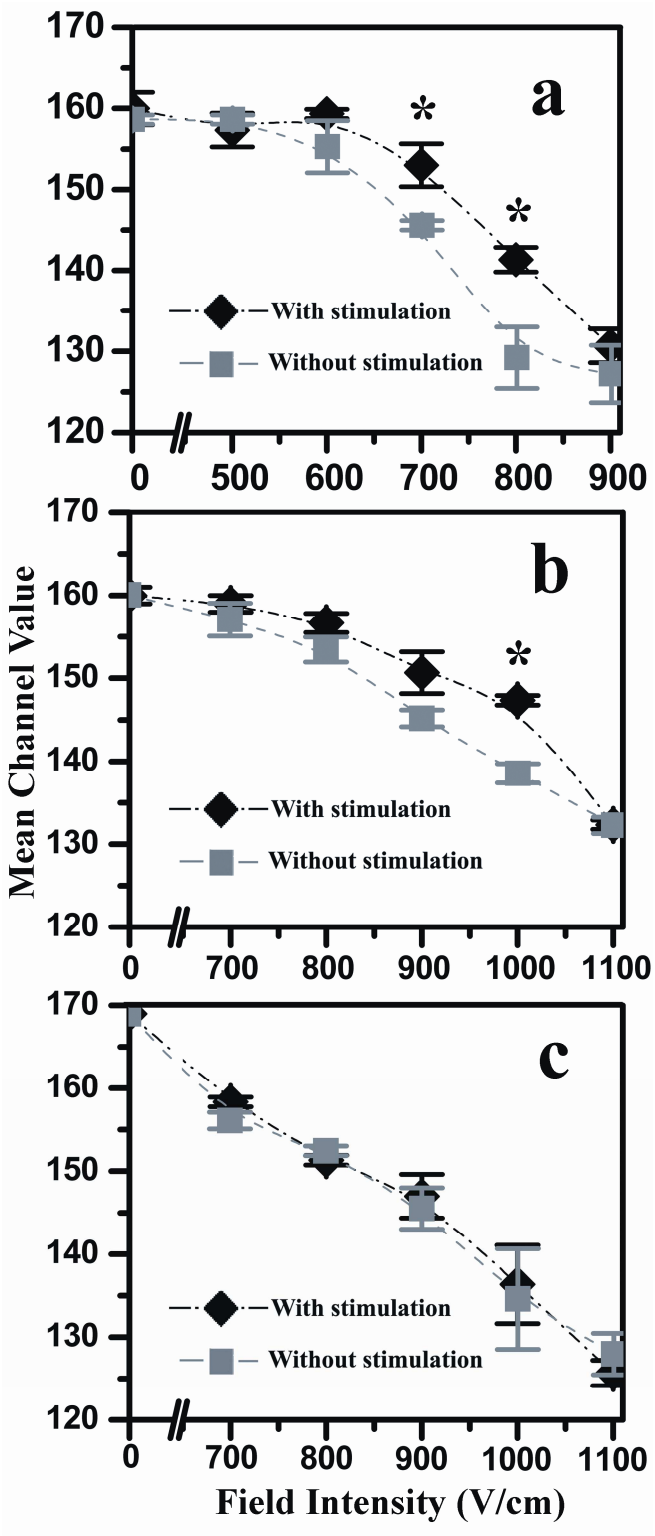

Figure 4. The variation of the mean fluorescence intensity value of the cell population at different field intensities with and without stimulation by anti-IgM. SykEGFP-DT40-Syk$^-$-Lyn$^-$ cells were applied in (**a**) and (**b**), while calcein AM stained DT40-Syk$^-$-Lyn$^-$ cells were used in (**c**). The data in (**a**) and (**b**) were obtained with different electroporation durations of 120 and 60 ms, respectively. The duration in (**c**) was 60 ms. The error bars were generated by carrying out the experiments in triplicate. (*) indicates significant difference at P<0.01, calculated using unpaired t test with equal variance.

IV. CONCLUSION

By combining electroporation with flow cytometry, we demonstrate microfluidic EFC as a new tool to differentiate cell populations with different activation states. Microfluidic EFC offers a simple and robust physical tool for detecting kinase translocation within the scope of the entire cell population. In principle, there are no intrinsic limitations that prevent our technology from having the throughput and the stability similar to those of

conventional flow cytometry. The time required for the electroporative release of the intracellular materials from cells does not necessarily put a limitation on the throughput. In principle, the length of the narrow section can be increased to maintain enough duration for the electroporative release of intracellular materials while both the throughput and the velocity of the cells are high. The microfluidic platform is well suited for both research and clinical settings.

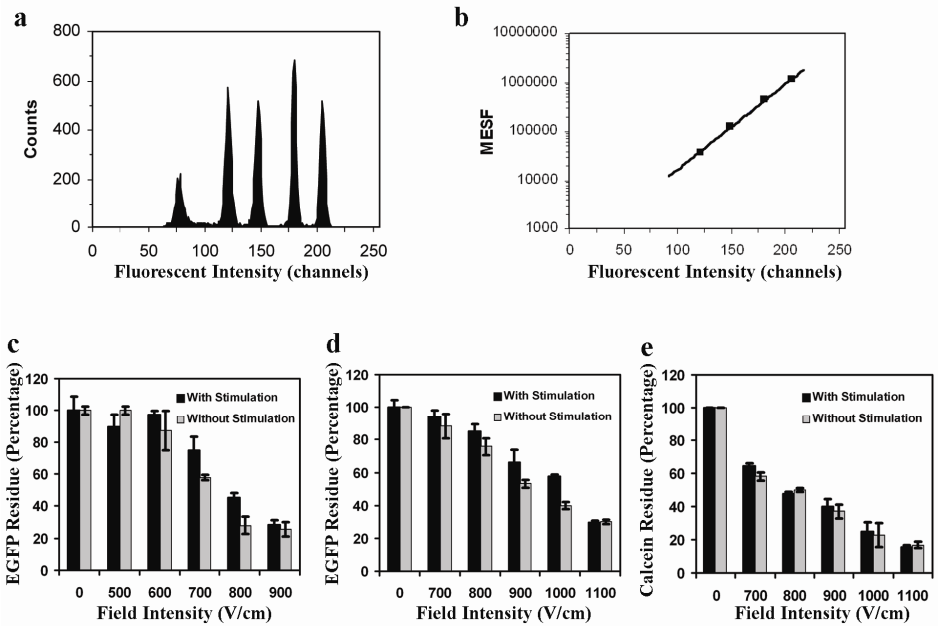

Figure 5. The quantitative analysis of the fluorescence intensity of DT40 cells. (**a**) The histogram of the fluorescence intensity from a mixture of beads with varying predefined fluorescence intensity levels. The data were generated by the microfluidic EFC system and the population with the lowest intensity is the reference blank. (**b**) The calibration curve with the MESF values of the beads plotted against the peak channel numbers (the fluorescent intensities) of the beads obtained by our microfluidic system (R^2=0.9978, solid square). The mean MESF value of the cells, $EGFP_{mean}$ in equation (5), is determined by finding the corresponding MESF value for a mean channel value known from the experiments. We assumed that the quantity of the fluorescent protein/calcein of the cell population detected by the system without the field (E = 0) was 100%. (**c**) The relative EGFP content in SykEGFP-DT40-Syk$^-$-Lyn$^-$ cells under different electric field intensities with a electroporation duration of 120 ms. (**d**) The relative EGFP content in SykEGFP-DT40-Syk$^-$-Lyn$^-$ cells under different electric field intensities with a electroporation duration of 60 ms. (**e**) The relative calcein content in calcein AM stained DT40-Syk$^-$-Lyn$^-$ under different electric field intensities with a electroporation duration of 60 ms.

V. ACKNOWLEDGEMENTS

We thank Purdue University and grant CA37372 from the National Cancer Institute for the financial support.

REFERENCES

1 Deptala, A., Bedner, E., Gorczyca, W. and Darzynkiewicz, Z. (1998) Activation of nuclear factor kappa B (NF-kappaB) assayed by laser scanning cytometry (LSC). *Cytometry* **33**, 376-382

2 Bedner, E., Li, X., Kunicki, J. and Darzynkiewicz, Z. (2000) Translocation of Bax to mitochondria during apoptosis measured by laser scanning cytometry. *Cytometry* **41**, 83-88

3 Ozawa, K., Hudson, C. C., Wille, K. R., Karaki, S. and Oakley, R. H. (2005) Development and validation of algorithms for measuring G-protein coupled receptor activation in cells using the LSC-based imaging cytometer platform. *Cytometry Part A* **65A**, 69-76

4 Wehrman, T. S., Casipit, C. L., Gewertz, N. M. and Blau, H. M. (2005) Enzymatic detection of protein translocation. *Nature Methods* **2**, 521-527

5 Rols, M. P. and Teissie, J. (1990) Electropermeabilization of mammalian cells. Quantitative analysis of the phenomenon. *Biophysical Journal* **58**, 1089-1098

6 Wang, H. Y. and Lu, C. (2006) Microfluidic chemical cytometry based on modulation of local field strength. *Chemical Communications*, 3528-3530

7 Wang, H. Y. and Lu, C. (2006) High-throughput and real-time study of single cell electroporation using microfluidics: effects of medium osmolarity. *Biotechnology and Bioengineering* **95**, 1116-1125

8 Wang, J. and Lu, C. (2006) Microfluidic cell fusion under continuous direct current voltage. *Applied Physics Letters* **89**, 234102

9 Takata, M. and Kurosaki, T. (1996) A role for Bruton's tyrosine kinase in B cell antigen receptor-mediated activation of phospholipase C-gamma 2. *Journal of Experimental Medicine* **184**, 31-40

10 Ma, H., Yankee, T. M., Hu, J. J., Asai, D. J., Harrison, M. L. and Geahlen, R. L. (2001) Visualization of Syk-antigen receptor interactions using green fluorescent protein: Differential roles for Syk and Lyn in the regulation of receptor capping and internalization. *Journal of Immunology* **166**, 1507-1516

11 Wang, L. L., Gaigalas, A. K., Abbasi, F., Marti, G. E., Vogt, R. F. and Schwartz, A. (2002) Quantitating fluorescence intensity from fluorophores: Practical use of MESF values. *Journal of Research of the National Institute of Standards and Technology* **107**, 339-353

12 Martin, B. R., Giepmans, B. N. G., Adams, S. R. and Tsien, R. Y. (2005) Mammalian cell-based optimization of the biarsenical-binding tetracysteine motif for improved fluorescence and affinity. *Nature Biotechnology* **23**, 1308-1314

13 Wang, H. Y. and Lu, C. (2006) Electroporation of mammalian cells in a microfluidic channel with geometric variation. Analytical Chemistry **78**, 5158-5164

14 Wang, J., Lu, C. (2006) Microfluidic cell fusion under continuous direct current voltage. *Applied Physics Letters* **89**, 234102